Helgoland Marine Research

ORIGINAL ARTICLE

Open Access

In the Asia-Pacific region, the COI DNA test revealed the divergence of the bivalve mollusc *Mactra chinensis* into three species; can these species be distinguished using shell coloration and sperm structure?

Arkadiy Reunov[1,2*], Konstantin Lutaenko[2], Evgenia Vekhova[2], Junlong Zhang[3], Evgeny Zakharov[4], Svetlana Sharina[2,5], Yana Alexandrova[2], Yulia Reunova[2], Anna Akhmadieva[2] and Andrey Adrianov[2,5]

Abstract

According to COI DNA barcoding testing, the marine bivalve mollusc *Mactra chinensis*, which is native to the Asia-Pacific region, diverged into three species. These species were preliminary characterized as *M. chinensis* COI clade I, *M. chinensis* COI clade II and *M. chinensis* COI clade III. To find out whether it is possible to morphologically distinguish samples representing genetic clades, we examined the color of the shells and the structure of the spermatozoa. It was found that the number of detected coloration types exceeds the number of detected species. In addition, it was shown that individuals belonging to the same genetic clade can have shells of different colors. Consequently, it is impossible to choose one type of shell coloration as a species-specific trait. For sperm, the sperm morphological patterns found in each of the three species are consistent with the *M. chinensis* sperm model described in previous reports. However, the single sperm variant is also not applicable to discriminate between species derived from *M. chinensis*, since heterogeneous variants of spermatozoa differing in the length of the acrosomal rod were found. We hypothesized that genetic divergence of species could cause a shift towards predominance of one of the sperm variants, and that species-specific sperm morphs could be quantitatively dominant in molluscs belonging to different clades. However, the dominant sperm morphs were the same in COI clade I and COI clade III. Thus, dominant sperm morphs are useless as species-specific traits. However, shell color and sperm parameters are specific to different geographic regions, and it seems that unique environmental factors can determine shell color and sperm morphology. As a result, both shells and spermatozoa can be used to distinguish the geographical forms of *M. chinensis*, regardless of the belonging of the forms to a particular genetic clade. Here we propose the introduction of geographic identifiers, in which the shell color and parameters of sperm sets are used as morphological criteria to determine the geographical origin of mollusc specimens belonging to the *M. chinensis* species complex.

Keywords: Pacific Ocean, *Mactra chinensis*, COI, DNA barcoding, Shell coloration, Sperm structure

Introduction

Bivalve molluscs of the family Mactridae Lamarck, 1809, the so-called "surf clams", inhabit the Asia-Pacific region along the coasts of Russia, Japan, Korea and China [1–10]. One of the mactrid species, *Mactra*

*Correspondence: areunov@stfx.ca
[1] Department of Biology, St. Francis Xavier University, Antigonish NS B2G 2W5, Canada
Full list of author information is available at the end of the article

chinensis Philippi, 1846, plays an important role in the production of seafood [11, 12]. In addition, *M. chinensis* is a rich source of keratin sulfate, glycosaminoglycan, useful for stimulating neuronal development, nerve growth and repairing damaged areas of the human nervous system, as well as for preventing Alzheimer's disease [13, 14].

For many years, the identification of *M. chinensis* was carried out only on the basis of morphological characters. The first test of the nucleotide sequence of the mitochondrial COI gene, carried out at the Canadian DNA Barcoding Center (Canada), showed that there are three clades of *M. chinensis*, such as clade COI I, clade COI II and clade COI III, which constitute separate species inhabiting the Russian, South Korean and Chinese parts of the Asia-Pacific region [15]. A second test, carried out at the Institute of Oceanology of the Chinese Academy of Sciences (China), confirmed this conclusion (present report). Thus, *M. chinensis* is thought to be a complex of three species. Since there are no new names for these new species yet, we preliminarily characterized them as *M. chinensis* COI clade I, *M. chinensis* COI clade II, and *M. chinensis* COI clade III.

The existence of three species implies the possibility of interspecies differences in pharmacological value. Therefore, an accurate definition of the species is important. For greater convenience, it would be important to find out whether the genetic varieties of *M. chinensis* differ morphologically.

It has been reported that shells of different colors can be found in northern and southern populations of *M. chinensis* in the Sea of Japan [15]. With this in mind, it would be logical to find out if there are three variants of shell coloration, each of which is typical for a particular species descended from *M. chinensis*. It would also be interesting to know if more than three shell coloration can be found among the *M. chinensis* species complex. Depending on how many color options are found, two possible reasons can be discussed that are likely to affect the shell color.

After the discovery of three genetic species of *M. chinensis*, it would be tempting to suggest that the plasticity of shell coloration may be associated with intraspecific divergence. A similar phenomenon was reported for *M. coralline*, in which the presence of two species which respectively have a white shell and a shell with brown rays was clearly confirmed by the analysis of genes 12S, 16S, 18S and COI [16]. However, it is also known that environmental factors can influence the coloration of mollusc shells [17]. Thus, more research is needed to understand which factor—intraspecific genetic divergence or environmental influences—is critical for determining the shell color of *M. chinensis*.

In addition to shells, an analysis of the structure of gametes can be used to detect divergence of the species. It has been established that, compared with the organism as a whole, reproductive cells undergo a faster rate of evolution and, therefore, different sperm morphology found in remote geographical populations of the species is a sign of probable divergence and speciation [18]. In the study of male gametes in *M. chinensis*, living in the southern and northern regions of the Sea of Japan and belonging respectively to *M. chinensis* COI clade I and *M. chinensis* COI clade II, it was found that each male has not one, but three morphological sperm patterns. Moreover, different sperm morphs were quantitatively dominant in representatives of COI clade I and clade II. It has been hypothesized that genetic divergence of species may be responsible for a shift towards a predominance of one of the sperm variants [15]. Given that *M. chinensis* is genetically divided into three clades, a more detailed analysis of spermatozoa in samples representing *M. chinensis* COI clade III is needed to test whether male gametes may be specific in this clades.

The aim of this article was to analyze the shell coloration and structure of spermatozoa of three species derived from the marine bivalve mollusc *M. chinensis*. For shells, to test whether it is possible to distinguish between species by the shell color specific to each species, our experiments consisted of the following: (1) to find out if there are three types of shell coloration, each of which corresponds to one of the three genetic clades; (2) examine the coloration of shells in museums and examine the shells of all available specimens to see if more than three coloration can be found; (3) determine if more than one shell color can correspond to the same genetic clade; (4) use scuba diving to study the molluscs in their natural habitat and check if the coloration of the shells is consistent with the local environment. As for spermatozoa, in order to test whether spermatozoa can be used to distinguish between species derived from *M. chinensis*, we examined the structure of male gametes in specimens belonging to the species *M. chinensis* COI clade III, and combined this with data obtained earlier for species *M chinensis* COI clade I and *M. chinensis* COI clade II. We hope that our observations will help to draw a conclusion about the applicability of shells and spermatozoa as morphological characters suitable for distinguishing the forms of *M. chinensis* inhabiting the Asia-Pacific region.

Materials and methods

Sample collection

Samples of the bivalve mollusc *Mactra chinensis* Philippi, 1846, genetically corresponding to the species *M. chinensis* COI clade I and *M. chinensis* COI clade II, were collected in the "Russian" and "South Korean" regions of the

Sea of Japan according to the protocol that was previously described [15]. Samples genetically consistent with *M. chinensis* COI clade III were collected by a supplier in the Yellow Sea of China near Yantai City (exact location unknown) and delivered by the supplier to a fish market in Yantai City, where they were identified as *M. chinensis* and purchased by Dr. K. Lutaenko on July 7, 2018.

Study of shell coloration in museum collections

We studied samples of *M. chinensis* from the collection of the Zoological Museum of the Far Eastern Federal University (Vladivostok, Russia), collected by Dr. K. Lutaenko, as well as samples from the collection of the Marine Biological Museum of the Chinese Academy of Sciences (Qingdao, China), collected by Dr. J. Zhang.

Investigation of *M. chinensis* shell coloration by SCUBA

M. chinensis specimens were collected from Peter the Great Bay (Sea of Japan) in September 2020 by Dr. Yana Alexandrova. SCUBA work was done by professional marine biology divers of NSCMB FEB RAS (Vladivostok, Russia). The samples were obtained by manually loosening the bottom substrate at a depth of four meters at the sites of holes, presumably the outlets of siphons of inhabitants, which sometimes turned out to be *M. chinensis*. Coordinates were identified using manual profiler Cast Away ctd. (SonTek, USA). The shells were delivered to the laboratory, dried and photographed by Dr. Yana Alexandrova under the same lighting conditions.

Transmission electron microscopy

M. chinensis is a dioecious species. Cases of hermaphroditism are unknown. There is no sexual dimorphism in the color and morphology of the shells. We identified males by detecting sperm in cell suspension using light microscopy. Male gonads were dissected, cut into small pieces and fixed overnight in primary fixative containing 2.5% glutaraldehyde in 0.1 M cacodylate buffer (pH 7.4) with osmolarity 1100 mOsm adjusted by sodium chloride. Fixed tissues were washed in buffer, postfixed in 2% OsO_4 in sea water, rinsed in 0.1 M cacodylate buffer and distilled water, dehydrated in an ethanol series, infiltrated and embedded in Spurr's resin. Ultra-thin sections were mounted on slot grids that were coated with formvar film. Sections were stained with 2% alcoholic uranyl acetate and Reynolds lead citrate and investigated using a Zeiss Libra 120 transmission electron microscope (Carl Zeiss, Oberkochen, Germany) and a Philips 410 transmission electron microscope (Philips 123 Electronics, Eindhoven, Netherlands).

Scanning electron microscopy

As for transmission electron microscopy, males were identified by examining the cell suspension using light microscopy. Sperm suspension was collected, pipetted onto a Thermanox coverslip (Cat. #72280) and allowed to settle for 5 min. Coverslips with attached sperm cells were fixed overnight in 2.5% glutaraldehyde in 0.1 M cacodylate buffer (pH 7.4) with osmolarity 1100 mOsm adjusted with sodium chloride. Primary fixed materials were washed in 0.1 M cacodylate buffer (pH 7.4) and postfixed in 1% OsO_4 in sea water. After the following washing in buffer, the samples were rinsed in distilled water, dehydrated in a graded series of ethanol solutions, transferred to acetone and critical-point dried in CO_2. Dried materials were mounted onto aluminum stubs, coated with gold, and examined with a scanning electron microscope LEO-430 (Horus Tech Inc., USA).

Quantitative analysis of sperm morphs

Two samples were taken from three geographic areas such as (i) the Sea of Japan "Vostok" Biological Station (Russia), (ii) the Sea of Japan, Gyeongsanbuk Province, Uljin County (South Korea), and (iii) the Yellow Sea near city Yantai (China). 500 sperm cells of each sample were evaluated, thus 1000 cells were studied from each geographic area, 3000 sperm cells altogether. Sperm phenotypes were identified by scanning electron microscopy, and the frequency of each phenotype was calculated. The results were analysed by the Microsoft Excel program. All values are expressed as means with standard error of the mean (SEM). Percentages were calculated using the Student's t test and $^{*}P < 0.05$, $^{**}P < 0.001$ were considered statistically significant.

Genetic analysis

The COI gene analysis was originally carried out at the Canadian DNA Barcoding Center (Canada), and its methodological description can be found in our previous publication [15]. The second test was carried out at the Institute of Oceanology, Chinese Academy of Sciences (China). The protocol is shown below.

Standard DNA barcoding protocols were followed at all stages of the analysis, including DNA extraction, PCR and DNA sequencing. A piece of the mantle or muscle (3–5 mm^3) was taken from three molluscs living in the Russian part of the Sea of Japan, from two molluscs living in the South Korean part of the Sea of Japan and from eight molluscs living in the Yellow Sea (China). Tissue samples were then subjected to overnight lysis in CTAB buffer with proteinase K (Invitrogen) followed by DNA extraction on a glass-fiber membrane (PALL) using automated protocol. A 658-bp barcoge region of the mtDNA

gene COI was amplified using primer cocktails C_LepFolF + C_LepFolR and C_LepFolF + SipR1 (LepF1, ATTCAACCAATCATAAAGATATTGG and LepR1, TAAACTTCTGGATGTCCAAAAAATCA; LCO1490, GTCAACAAATCATAAAGATATTGG and HCO2198, TAAACTTCAGGGTGACCAAAAAATCA, SipR1, TAA ACTTCTGGRTGRCCAAARAAYCA).

The polymerase chain reaction (PCR) mix included 6.25 µl of 10% trehalose, 1.25 µl 10 × PCR buffer, 0.625 µl (2.5 mM) $MgCl_2$, 0.125 µl (10 µM) forward and reverse primer cocktail, 0.625 ul (10 mM) dNTPs, 0.625 µl Platinum Taq polymerase, 3 µl H_20 and 1 µl of DNA template. PCRs were run under the following cycle conditions: 1 min at 94 °C followed by 5 cycles of 30 s at 94 °C, 40 s at 55 °C, and 1 min at 72 °C, followed by 35 cycles of 30 s at 94 °C, 40 s at 55 °C, and 1 min at 72 °C, with final 10 min at 72 °C extension. PCR products were detective via agarose gel electrophoresis using buffer-less precast E-Gel system (Invitrogen). Successful amplicons were cycle sequenced using BigDye version 3.1 using manufacturer's recommended protocols. Sequencing products with incorporated BigDye terminator were purified using Edge AutoDTR96 kit (EdgeBio) and analyzed on ABI3730xl DNA sequencer.

ABI trace files for each specimen were assembled into contigs using Codon Code Aligner software. In addition to the 13 consensus sequences generated, DNA sequence data for *M. chinensis* and *Mactra* sp. collected from the Yellow Sea and the East China Sea [19, 20] and for some additional congeneric species in published papers [21, 22] were downloaded from Genbank and the BOLD Public Data Portal. The final dataset of 121 partial COI sequences was aligned by eye in BioEdit. All original specimen metadata, sequences, and trace files were uploaded to the Barcode of Life Data Systems (BOLD) at http://www.boldsystems.org or GenBank at https://www.ncbi.nlm.nih.gov/genbank/.

To discriminate species, the Automatic Barcode Gap Discovery (ABGD) analysis [23] were used to scan a range of prior intraspecific divergence from $P_{min} = 0.001$ to $P_{max} = 0.1$, with 10 steps, 1.5 for the minimum relative gap width, and using Jukes-Cantor (JC69) and Kimura (K80) measure of distance. Nucleotide sequence divergences were also calculated in MEGA X [24] using the Kimura two-parameter (K2P) nucleotide substitution model [25]. Sequences that were split into distinct groups with clear barcoding gaps are hypothesized to represent provisional species. The best-fitted evolutionary models were selected by AICc as implemented in jModeltest2 [26]. The general time-reversible substitution with discretized gamma-distributed rate and invariant sites model (GTR + G + I) was selected as the best-fitted model. Bayesian inference (BI) was conducted using the software MrBayes 3.2.6 [27]. Posterior probability (PP) was estimated using four chains running 10,000,000 generations sampling every 100 generations. Maximum likelihood (ML) analysis was carried out using RAxML 8.1.2 [28] (with bootstrapping) using GTR + G + I as the model. Node support came from the bootstrap scores (BS) in the best-scoring tree of 1,000 bootstrap replicates. The neighbor-joining phylogenetic tree [29] was inferred in MEGA X [24] using theK2P method [25] with the 1000 replicates bootstrap test. Results were visualized using FigTree v. 1.4.3.

Results

DNA COI testing

Samples of *M. chinensis* COI clade I, *M. chinensis* COI clade II, and *M. chinensis* COI clade III were taken from the "Russian", "South Korean" and "Chinese" regions of the Asia-Pacific region (Fig. 1). The following samples were analyzed; from the "Russian" area—three samples (YARRA073-12/RRYA-73; YARRA074-12/RRYA-74; YARRA075-12/RRYA-75) (Table 1, blue, column—"present study"); from the "South Korean" area—two samples (YARRA072-12/RRYA-72; YARRA071-12/RRYA-71) (Table 1, pink, column—"present study"); from the "Chinese" area—four samples (ABCBF460-19, ABCBF461-19, ABCBF462-19, ABCBF463-19) (Table 1, green, column—"present study").

Multiple polymorphic sites were detected in the alignment of sequence data for analyzed samples of the *M. chinensis* collected in the northern and southern areas of the Sea of Japan and in the Yellow Sea. No insertions or deletions have been detected. All nucleotide substitutions were silent (i.e., not resulting in any amino acid changes) and were observed largely in third codon positions. For the analysis of nucleotide

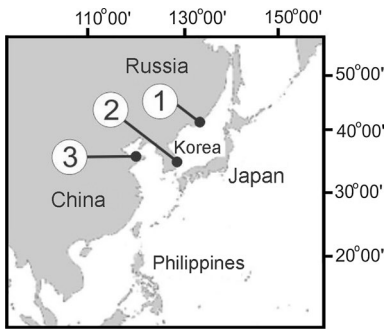

Fig. 1 General map of the Asia-Pacific region showing the habitats of three species resulting from the divergence of the bivalve mollusc *Mactra chinensis*. The species were identified by testing with COI DNA barcoding (17 and the present study); 1—*M. chinensis* COI clade I (Sea of Japan, Russia); 2—*M. chinensis* COI clade II (Sea of Japan, South Korea); 3—*M. chinensis* COI clade III (Yellow Sea, China)

Table 1 List of species, locality and their accession numbers of sequences used in present study

Species	Locality	Haplotype/Isolate/Sample	Accession numbers	References
Mactra chinensis	Sea of Japan, South Korea	RRYA-71	YARRA071-12	Present study
Mactra chinensis	Sea of Japan, South Korea	RRYA-72	YARRA072-12	Present study
Mactra chinensis	Sea of Japan, Russia	RRYA-73	YARRA073-12	Present study
Mactra chinensis	Sea of Japan, Russia	RRYA-74	YARRA074-12	Present study
Mactra chinensis	Sea of Japan, Russia	RRYA-75	YARRA075-12	Present study
Mactra chinensis	Yantai, Yellow Sea, China	CCDB-ST03126	ABCBF460-19	Present study
Mactra chinensis	Yantai, Yellow Sea, China	CCDB-ST03127	ABCBF461-19	Present study
Mactra chinensis	Yantai, Yellow Sea, China	CCDB-ST03128	ABCBF462-19	Present study
Mactra chinensis	Yantai, Yellow Sea, China	CCDB-ST03129	ABCBF463-19	Present study
Mactra chinensis	Rushan, Yellow Sea, China	MAR1	MT791493	Present study
Mactra chinensis	Rushan, Yellow Sea, China	MAR2	MT791494	Present study
Mactra chinensis	Rushan, Yellow Sea, China	MAR4	MT791495	Present study
Mactra chinensis	Rushan, Yellow Sea, China	MAR5	MT791496	Present study
Mactra chinensis	Yellow Sea, China	1	KC205870	Ni et al., 2015
Mactra chinensis	Yellow Sea, China	2	KC205871	Ni et al., 2015
Mactra chinensis	Yellow Sea, China	3	KC205872	Ni et al., 2015
Mactra chinensis	Yellow Sea, China	4	KC205873	Ni et al., 2015
Mactra chinensis	Yellow Sea, China	5	KC205874	Ni et al., 2015
Mactra chinensis	Yellow Sea, China	6	KC205875	Ni et al., 2015
Mactra chinensis	Yellow Sea, China	7	KC205876	Ni et al., 2015
Mactra chinensis	Yellow Sea, China	8	KC205877	Ni et al., 2015
Mactra chinensis	Yellow Sea, China	9	KC205878	Ni et al., 2015
Mactra chinensis	Yellow Sea, China	10	KC205879	Ni et al., 2015
Mactra chinensis	Yellow Sea, China	11	KC205880	Ni et al., 2015
Mactra chinensis	Yellow Sea, China	12	KC205881	Ni et al., 2015
Mactra chinensis	Yellow Sea, China	13	KC205882	Ni et al., 2015
Mactra chinensis	Yellow Sea, China	14	KC205883	Ni et al., 2015
Mactra chinensis	Yellow Sea, China	15	KC205884	Ni et al., 2015
Mactra chinensis	Yellow Sea, China	16	KC205885	Ni et al., 2015
Mactra chinensis	Yellow Sea, China	17	KC205886	Ni et al., 2015
Mactra chinensis	Yellow Sea, China	18	KC205887	Ni et al., 2015
Mactra chinensis	Yellow Sea, China	19	KC205888	Ni et al., 2015
Mactra chinensis	Yellow Sea, China	20	KC205889	Ni et al., 2015
Mactra chinensis	Yellow Sea, China	21	KC205890	Ni et al., 2015
Mactra chinensis	Yellow Sea, China	22	KC205891	Ni et al., 2015
Mactra chinensis	Yellow Sea, China	23	KC205892	Ni et al., 2015
Mactra chinensis	Yellow Sea, China	24	KC205893	Ni et al., 2015
Mactra chinensis	Yellow Sea, China	25	KC205894	Ni et al., 2015
Mactra chinensis	Yellow Sea, China	26	KC205895	Ni et al., 2015
Mactra chinensis	Yellow Sea, China	27	KC205896	Ni et al., 2015
Mactra chinensis	Yellow Sea, China	28	KC205897	Ni et al., 2015
Mactra chinensis	Yellow Sea, China	29	KC205898	Ni et al., 2015
Mactra chinensis	Yellow Sea, China	30	KC205899	Ni et al., 2015
Mactra chinensis	Yellow Sea, China	31	KC205900	Ni et al., 2015
Mactra chinensis	Yellow Sea, China	32	KC205901	Ni et al., 2015
Mactra chinensis	Yellow Sea, China	33	KC205902	Ni et al., 2015
Mactra chinensis	Yellow Sea, China	34	KC205903	Ni et al., 2015
Mactra chinensis	Yellow Sea, China	35	KC205904	Ni et al., 2015
Mactra chinensis	Yellow Sea, China	36	KC205905	Ni et al., 2015
Mactra chinensis	Yellow Sea, China	37	KC205906	Ni et al., 2015
Mactra chinensis	Yellow Sea, China	38	KC205907	Ni et al., 2015

Table 1 (continued)

Mactra chinensis	Yellow Sea, China	39	KC205908	Ni et al., 2015
Mactra chinensis	Yellow Sea, China	40	KC205909	Ni et al., 2015
Mactra chinensis	Yellow Sea, China	41	KC205910	Ni et al., 2015
Mactra chinensis	Yellow Sea, China	42	KC205911	Ni et al., 2015
Mactra chinensis	Yellow Sea, China	43	KC205912	Ni et al., 2015
Mactra chinensis	Yellow Sea, China	44	KC205913	Ni et al., 2015
Mactra chinensis	Yellow Sea, China	45	KC205914	Ni et al., 2015
Mactra chinensis	Yellow Sea, China	46	KC205915	Ni et al., 2015
Mactra chinensis	Yellow Sea, China	47	KC205916	Ni et al., 2015
Mactra chinensis	Yellow Sea, China	48	KC205917	Ni et al., 2015
Mactra chinensis	East China Sea, China	49	KC205918	Ni et al., 2015
Mactra chinensis	East China Sea, China	50	KC205919	Ni et al., 2015
Mactra chinensis	East China Sea, China	51	KC205920	Ni et al., 2015
Mactra chinensis	East China Sea, China	52	KC205921	Ni et al., 2015
Mactra chinensis	East China Sea, China	53	KC205922	Ni et al., 2015
Mactra chinensis	East China Sea, China	54	KC205923	Ni et al., 2015
Mactra chinensis	East China Sea, China	55	KC205924	Ni et al., 2015
Mactra chinensis	East China Sea, China	56	KC205925	Ni et al., 2015
Mactra chinensis	East China Sea, China	57	KC205926	Ni et al., 2015
Mactra chinensis	Pingtan, East China Sea, China	Z1	JN674630	Ni et al., 2012
Mactra chinensis	Lianyungang, Yellow Sea, China	Z2	JN674631	Ni et al., 2012
Mactra chinensis	Wendeng, Yellow Sea, China	Z3	JN674632	Ni et al., 2012
Mactra chinensis	Qinhuangdao, Yellow Sea, China	Z4	JN674633	Ni et al., 2012
Mactra chinensis	Dandong, Yellow Sea, China	Z5	JN674634	Ni et al., 2012
Mactra chinensis	Nanji, East China Sea, China	Z6	JN674635	Ni et al., 2012
Mactra sp.	Dandong, Yellow Sea, China	CX1	JN674626	Ni et al., 2012
Mactra sp.	Dandong, Yellow Sea, China	CX2	JN674627	Ni et al., 2012
Mactra sp.	Dandong, Yellow Sea, China	CX3	JN674628	Ni et al., 2012
Mactra sp.	Dandong, Yellow Sea, China	CX4	JN674629	Ni et al., 2012
Mactra mauclata	Wenchang, Hainan, China	B1	JN674613	Ni et al., 2012
Mactra mauclata	Wenchang, Hainan, China	B2	JN674614	Ni et al., 2012
Mactra alta	Beihai, Guangxi, China	GGL1	JN674615	Ni et al., 2012
Mactra alta	Beihai, Guangxi, China	GGL2	JN674616	Ni et al., 2012
Mactra alta	Beihai, Guangxi, China	GGL3	JN674617	Ni et al., 2012
Mactra alta	Beihai, Guangxi, China	GGL4	JN674618	Ni et al., 2012
Mactra alta	Beihai, Guangxi, China	GGL5	JN674619	Ni et al., 2012
Mactra alta	Beihai, Guangxi, China	GGL6	JN674620	Ni et al., 2012
Mactra veneriformis	Lianyungang, Jiangsu, China	S1	JN674621	Ni et al., 2012
Mactra veneriformis	Zhoushan, Zhengjiang, China	S2	JN674622	Ni et al., 2012
Mactra veneriformis	Beihai, Guangxi, China	S3	JN674623	Ni et al., 2012
Mactra veneriformis	Dalian, Liaoning, China	S4	JN674624	Ni et al., 2012
Mactra veneriformis	Dongying, Shandong, China	S5	JN674625	Ni et al., 2012
Mactra corallina	Tunisia	HMA1	KM673272	Chetoui et al., 2016
Mactra corallina	Tunisia	HMA2	KM673273	Chetoui et al., 2016
Mactra corallina	Tunisia	HMA3	KM673274	Chetoui et al., 2016
Mactra corallina	Tunisia	HMA4	KM673275	Chetoui et al., 2016
Mactra corallina	Tunisia	HMA5	KM673276	Chetoui et al., 2016
Mactra corallina	Tunisia	HMA6	KM673277	Chetoui et al., 2016
Mactra corallina	Tunisia	HMA7	KM673278	Chetoui et al., 2016

Table 1 (continued)

Mactra corallina	Tunisia	HMA8	KM673279	Chetoui et al., 2016
Mactra corallina	Tunisia	HMA9	KM673280	Chetoui et al., 2016
Mactra corallina	Tunisia	HMA10	KM673281	Chetoui et al., 2016
Mactra corallina	Tunisia	HMA11	KM673282	Chetoui et al., 2016
Mactra corallina	Tunisia	HMA12	KM673283	Chetoui et al., 2016
Mactra corallina	Tunisia	HMA13	KM673284	Chetoui et al., 2016
Mactra corallina	Tunisia	HMA14	KM673285	Chetoui et al., 2016
Mactra corallina lignaria	Cesenatico, Italy	3	FJ830435	Guarniero et al., 2010
Mactra corallina lignaria	Cesenatico, Italy	10	FJ830436	Guarniero et al., 2010
Mactra corallina lignaria	Cesenatico, Italy	22	FJ830437	Guarniero et al., 2010
Mactra corallina lignaria	Cesenatico, Italy	23	FJ830438	Guarniero et al., 2010
Mactra corallina lignaria	Cesenatico, Italy	25	FJ830439	Guarniero et al., 2010
Mactra corallina lignaria	Cesenatico, Italy		GQ166586	Plazzi and Passamonti, 2010
Mactra corallina	Cesenatico, Italy	5	FJ830440	Guarniero et al., 2010
Mactra corallina	Cesenatico, Italy	10	FJ830441	Guarniero et al., 2010
Mactra corallina	Cesenatico, Italy	19	FJ830442	Guarniero et al., 2010
Mactra corallina	Cesenatico, Italy	21	FJ830443	Guarniero et al., 2010
Mactra corallina	Cesenatico, Italy	30	FJ830444	Guarniero et al., 2010
Mactra corallina	Cesenatico, Italy	31	FJ830445	Guarniero et al., 2010
Mactra corallina	Cesenatico, Italy	32	FJ830446	Guarniero et al., 2010
Mactra corallina	Cesenatico, Italy		GQ166585	Plazzi and Passamonti, 2010

sequences, we used DNA barcoding of the materials collected by us and the data retrieved from Genebank. Total of 121 partial COI sequences were used for genetic analysis (Table 1).

The ABGD analysis based on the COI alignment using the Jukes-Cantor (JC69) and Kimura (K80) models yields 10 distinct groups, which represent 10 candidate species (Fig. 2). Pairwise K2P distances of COI within the 10 groups are much lower (0–0.0206) than those between groups (0.0820–0.2894) (Table 2). There is no overlap but clear barcoding gap between intra- and inter-specific distances of all candidate species. That support the validity of these 10 candidate species.

The phylogenetic trees established using BI, ML and NJ analyses are generally consistent. Thus, a single topology is presented with support values indicated on branches (Fig. 2). In the trees, the 10 species form separate clades, with *M. chinensis* splits into three clades. The first clade is represented by haplotypes shared by *M. chinensis* specimens from the northern part (Russia) of the Sea of Japan (YARRA074-12/RRYA-74; YARRA075-12/RRYA-75; YARRA073-12/RRYA-73) and *Mactra* sp. samples from the northern part of the Yellow Sea (individuals CX2, CX3, and CX4 in [19]). The second clade includes haplotypes shared by the specimens from the southern part (South Korea) of the Sea of Japan (YARRA072-12/

(See figure on next page.)

Fig. 2 Phylogenetic trees inferred by Bayesian analysis (BI), maximum likelihood (ML) and neighbor-joining (NJ) of *Mactra chinensis* and congeneric species based on available sequence data from the barcode region of mtDNA gene COI. Numbers adjacent to nodes refer to BI posterior probability (PP), ML bootstrap scores (BS) and NJ bootstrap scores (BS). Different candidate species inferred from Automatic Barcode Gap Discovery (ABGD) analysis were grouped by bars beside the sequences. The sequences resulting from this study are shown in bold. Clades of *M. chinensis* are marked with different colors; blue (COI clade I)—samples collected in the Sea of Japan (Russia) (YARRA073-12/RRYA-73; YARRA074-12/RRYA-74; YARRA075-12/RRYA-75;); pink (COI clade II)—samples collected in the Gyeongsanbuk region of the Sea of Japan (South Korea) (YARRA071-12/RRYA-71; YARRA072-12/RRYA-72); green (COI clade III)—samples collected in the Yantai area of Yellow Sea (China) (ABCBF460-19, ABCBF461-19, ABCBF462-19, ABCBF463-19). Note the samples collected in the Yellow Sea near Yantai (green and bold—ABCBF460-19, ABCBF461-19, ABCBF462-19, ABCBF463-19) and samples collected in the Yellow Sea near Weihai (green and bold—MT791493, MT791494, MT791495, MT791496), which belong to one clade (COI clade III; green color)

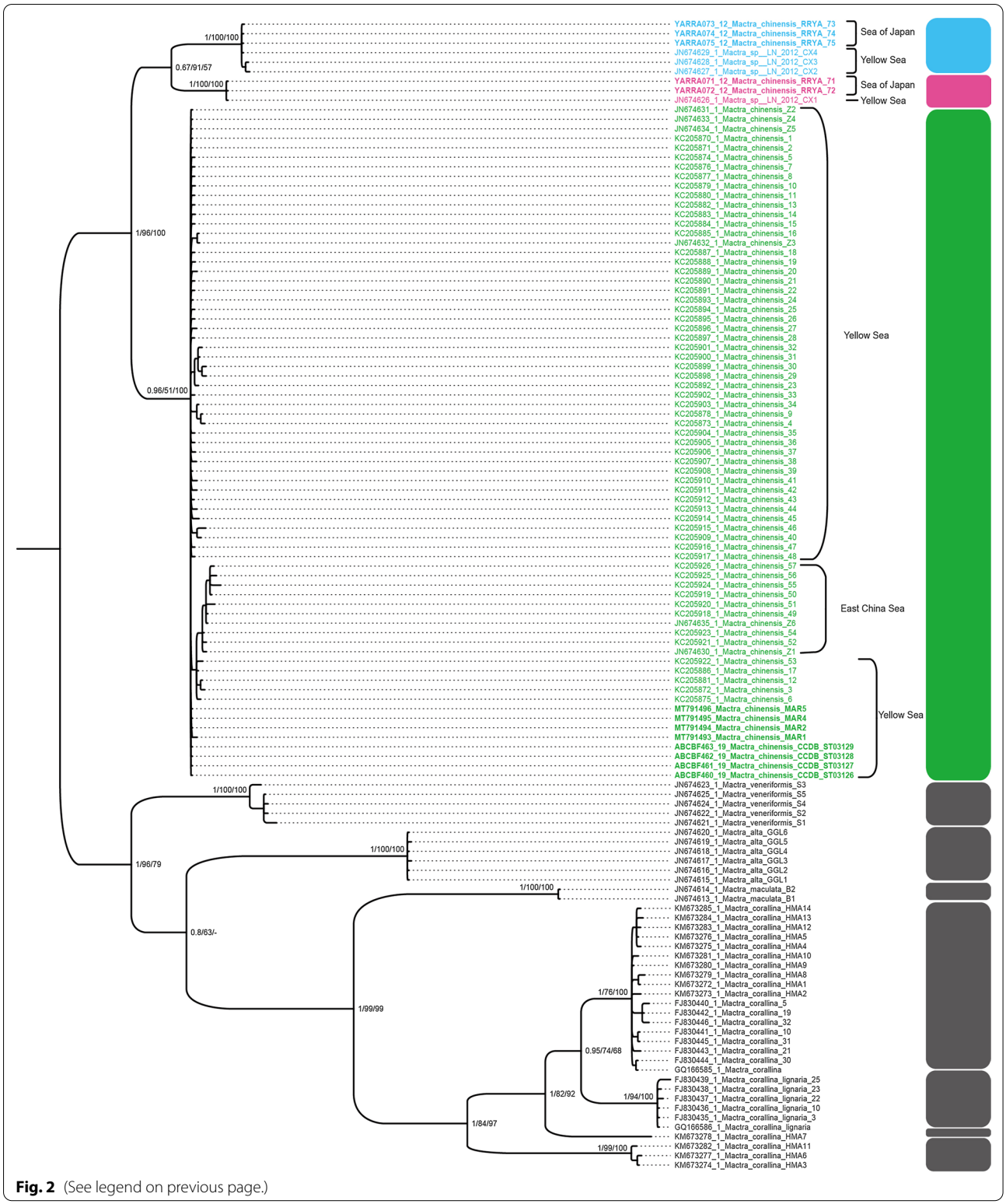

Fig. 2 (See legend on previous page.)

RRYA-72; YARRA071-12/RRYA-71) and *Mactra* sp. samples from the Yellow Sea (CX1 in [19]. The third clade represents *M. chinensis* haplotypes shared by samples collected in the Yellow Sea (ABCBF460-19, ABCBF461-19, ABCBF462-19, ABCBF463-19; MAR1; MAR2; MAR4; MAR5; Specimens Z2–Z5 in [19]; Haplotype

Table 2 Pairwised Kimura 2-parameter (K2P) distances at COI within and between the ABGD groups

Group	Candidate species	I	II	III	IV	V	VI	VII	VIII	IX	X
I	*M. chinensis* clade I	0.0000–0.0033									
II	*M. chinensis* clade II	0.0820–0.0880	0.0000–0.0000								
III	*M. chinensis* clade III	0.0954–0.1159	0.0824–0.0989	0.0000–0.0278							
IV	*M. veneriformis*	0.1547–0.1678	0.1834–0.1924	0.1557–0.1751	0.0016–0.0206						
V	*M. alta*	0.2006–0.2191	0.2177–0.2305	0.2173–0.2408	0.1791–0.1945	0.0000–0.0032					
VI	*M. maculata*	0.2337–0.2420	0.2307–0.2352	0.2219–0.2407	0.2288–0.2369	0.2712–0.2792	0.0000–0.0000				
VII	*M. corallina* clade I	0.2333–0.2542	0.2394–0.2476	0.2088–0.2423	0.2118–0.2266	0.2597–0.2878	0.2141–0.2259	0.0000–0.0178			
VIII	*M. corallina lignaria*	0.2497–0.2632	0.2528–0.2634	0.2371–0.2817	0.2216–0.2315	0.2762–0.2844	0.2286–0.2286	0.1648–0.1719	0.0000–0.0124		
IX	*M. corallina* clade II	0.2492–0.2542	0.2545–0.2545	0.2473–0.2803	0.2337–0.2385	0.2776–0.2812	0.2068–0.2068	0.1161–0.1274	0.1253–0.1322	c/n	
X	*M. corallina* clade III	0.2247–0.2366	0.2720–0.2747	0.2465–0.2614	0.2128–0.2247	0.2781–0.2894	0.2345–0.2392	0.1659–0.1818	0.1648–0.1719	0.1790–0.1834	0.0017–0.0068

1–48 in [21]) and specimens from the East China Sea (including specimens Z1 and Z6 in [29]; Haplotype 49–57 in [20]. Thus, the analysis confirmed the existence of three COI lines of the species *M. chinensis*.

Shell coloration of genetically tested samples

Shells of genetically tested samples collected in the Vostok Bay of the Sea of Japan (Russia) (YARRA074-12/RRYA-74; YARRA075-12/RRYA-75; YARRA073-12/RRYA-73), have rays radially extending from the beak, and have a lilac hue with a point of view of the general tone (Fig. 3-1).

Shells of genetically tested samples collected in the Gyeongsanbuk region of the Sea of Japan (South Korea) (YARRA071-12/RRYA-71; YARRA072-12/RRYA-72) are brownish with a bright beak and radially extending rays that are not clearly visible (Fig. 3-2).

Shells of genetically tested samples collected in the Yantai area of Yellow Sea (China) (ABCBF460-19, ABCBF461-19, ABCBF462-19, ABCBF463-19) have rays radially extending from the beak, but look mustard in terms of overall tone (Fig. 3-3).

Shell coloration of museum samples

Work in the museum collections showed that other shell colors are present in *M. chinensis*. For example, the malacological collection of the Zoological Museum of the Far Eastern Federal University (Vladivostok, Russia) contains shells from the Ussuriisky Bay (Sea of Japan, Russia), which have brightly visible violet–purple rays against a light background, and the edge of the shell also has a purple color (Fig. 3-4). Shell samples collected in the Gyeonsang area of South Korean part of the Sea of Japan are devoid of any rays and have pale yellow tones (Fig. 3-5). Dr. J. Zhang's collection contains shell specimens collected in the Yellow Sea of China, which are represented by two variants from Qingdao, one of which is devoid of any rays and has a pale pink tint (Fig. 3-6), and another has very light ochroid tone with slightly visible stripes (Fig. 3-7). In the same collection, one can see two variants of mactra from Weihai, which are distinguished by a dark and pale ocher shade (Fig. 3-8, 9). The same collection has four variants of mactra from the Bohai Sea in China, which are represented by two variants from Qinghuangdao, which have a pearlescent hue and differing intensity of ocher stripes (Fig. 3-10, 11), and two very different variants from Beidaihe, one of which is specimen showing irregular ocher tone and another white with ocher stripes on it (Fig. 3-12, 13). Also, the collection of Dr. J. Zhang allows to see two samples of *M. chinensis* collected in the East China Sea near Pingtan (China). One of these is stripe-less with very light ochroid tone and another has pale ochroid stripes on the pearly background (Fig. 3-14, 15).

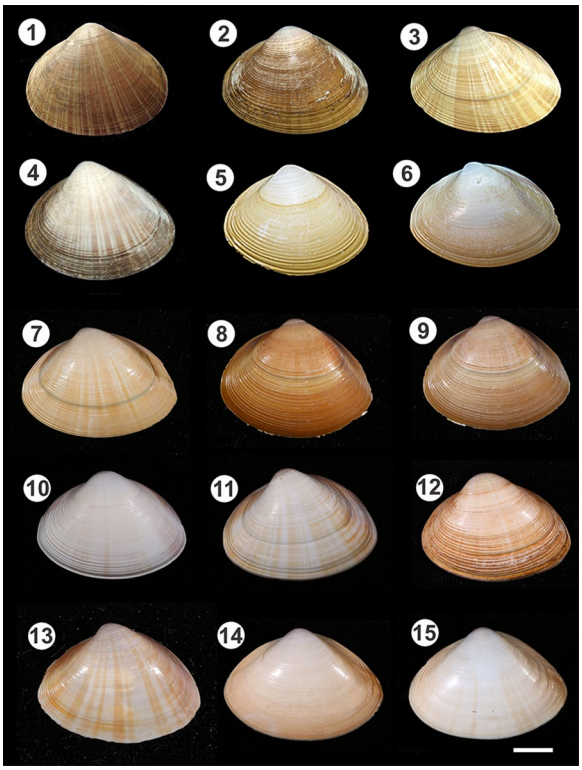

Fig. 3 Intraspecific variations in the external coloration of the shells of the bivalve mollusc *Mactra chinensis*; 1—The Sea of Japan,Vostok bay, Russia; collected and stored by Dr. Y. Alexandrova. 2—The Sea of Japan Gyeongsanbuk Province, Uljin County (Uljin-gun), South Korea; collected and stored by Dr. K. Lutaenko. 3—Yellow Sea, Yantai, China; collected and stored by Dr. K. Lutaenko. 4—The Sea of Japan, Ussurian bay, Russia; collection of the Zoological Museum of the Far Eastern Federal University (ZMFU). 5—The Sea of Japan, Gyeonsang, South Korea; collection of the Zoological Museum of the ZMFU. 6—Yellow sea, Qingdao, China; collection of the Zoological Museum of the ZMFU. 7—Yellow sea, Qingdao, China; Collection of Dr. J. Zhang. 8—Yellow sea, Ruhan (Weihai), China; Collection of Dr. J. Zhang. 9—Yellow sea, Ruhan (Weihai), China; Collection of Dr. J. Zhang. 10—Bohai Sea, Qinghuangdao, China; Collection of Dr. J. Zhang. 11—Bohai Sea, Qinghuangdao, China; Collection of Dr. J. Zhang. 12—Bohai Sea, Beidaihe, China; Collection of Dr. J. Zhang. 13—Bohai Sea, Beidaihe, China; Collection of Dr. J. Zhang. 14—East-China Sea, Pingtan, China; Collection of Dr. J. Zhang. 15—East-China Sea, Pingtan, China; Collection of Dr. J. Zhang. Scale bar = 1 sm

Investigation of the shell color in samples belonging to the COI clade III

In this part of the study, we used data of Dr. J. Zhang to test if the shell colors are similar in *M. chinensis* specimens belonging to the same COI clade (sperms were not examined). Samples collected in the Yellow Sea near Yantai (ABCBF460-19, ABCBF461-19, ABCBF462-19,

ABCBF463-19) and samples collected in the Yellow Sea near Weihai (MT791493, MT791494, MT791495, MT791496) were genetically matched and belonging of all samples to one clade (COI of clade III) was confirmed (Table 1; Fig. 2). Shell coloration of all samples was morphologically compared. Morphologic analyses of the Yantai's *M. chinensis* samples showed that their shells have characteristic rays radially extending from the beak, and colored in mustard-like overall tone having slight intensity variations between the samples (Fig. 4-1–4). Samples collected near Rushan show variations in brownish tone, which can be bright (Fig. 4-5) or relatively pale (Fig. 4-6–8), as well as vary from a very weak tone of the rays (Fig. 4-5, 6) to relatively bright rays (Fig. 4-7, 8). In any case, each group of specimens is specific in terms of overall hue, and shells from Yantai and Rushan can be classified into shells having a mustard tone and shells having a brownish tone.

Shell coloration of *M. chinensis* collected by SCUBA in the natural environment

Samples of *M. chinensis* were collected from four sites in Peter the Great Bay (Fig. 5-1–4). The shell periostracum of some samples looked fade or damaged. However, we managed to find samples that have a normal state of color, or we used unchanged pigment areas on the shells. Given that some tone differences were obvious between the central areas of shells (red squares at Fig. 6A-1–3; B-1–3; C-1–3; D-1–3) and marginal areas of shells (yellow squares at Fig. 6A-1–3; B-1–3; C-1–3; D-1–3), we considered both the marginal shell colours and central ones. The squares representing central and marginal shell areas were combined correspondingly to each of three typical samples that were choosen for demonstration from the samples found in the collection point #1 (Fig. 6A′-1,1′; 2,2′; 3,3′), collection point #2 (Fig. 6B′-1,1′; 2,2′; 3,3′), collection point #3 (Fig. 6C′-1,1′; 2,2′; 3,3′) and collection point #4 (Fig. 6D′-1,1′; 2,2′; 3,3′).

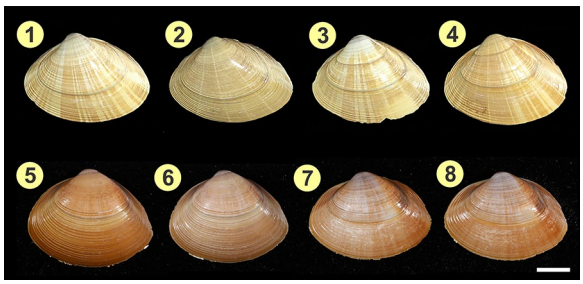

Fig. 4 Mustard (1–4) and brownish (5–8) shell colors found in samples of the bivalve mollusc *Mactra chinensis* belonging to the same genetic clade (clade COI III); collection of Dr. J. Zhang. 1–4 correspond to samples collected in the Yellow Sea near Yantai (ABCBF460-19, ABCBF461-19, ABCBF462-19, ABCBF463-19) (Table 1, green, column—'present study; Fig. 2, green and bold), and 5–8 correspond to samples collected in the Yellow Sea near Weihai (MT791493, MT791494, MT791495, MT791496) (Table 1, green, column—'present study'; Fig. 2, green and bold). Scale bar = 1 sm

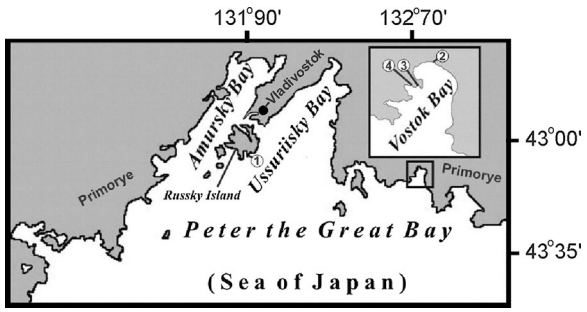

Fig. 5 Map of Peter the Great Bay (Sea of Japan, Russia) showing the geographical collection points (1–4) of *Mactra chinensis* specimens whose shells were used for in vivo color analysis during SCUBA diving. 1—Russky Island, Vyatlin Cape (coordinates of the gathering place—42°57′58.68″N, 131°54′09.7″E); 2—Vostok Bay, Volchanets town (coordinates of the gathering place—42°54′20, 52″N, 132°45″28.8″E); 3—Vostok Bay, Pervaya Priboynaya Bay (coordinates of the gathering place—42°53′11.4″N, 132°43′40.8″E); 4—Vostok Bay, Vtoraya Priboynaya Bay (coordinates of the gathering place—42°53′12.48′N, 132°43′18.48″E)

In the collection point #1 (Fig. 5-1), the water temperature and salinity of sea water were 19.99 °C and 31.75‰ respectively. Some shells have damaged periostracum (Fig. 6A-1) but another shells appear normal (Fig. 6A-2, 3). Shells usually have stripes (Fig. 6A-1–3). The central shell areas are stained in either dark brownish-terracotta pigment (Fig. 6A′-1), or in slightly red terracotta pigments (Fig. 6A′-2, 3). Periferal areas of shells are stained in the same brownish-terracotta colour but appear more light comparatively to the central areas and are peculiar in having contrasted stripes (Fig. 6A′-1′–3′). Most typical brownish-terracotta pigment is represented by a periostracum piece taken from the central shell area of one of the mollucs (Fig. 6A″). The sand of the sea bottom substrate was found to have a grayish-brown tone (Fig. 6A‴).

In the collection point #2 (Fig. 5-2), the water temperature and salinity were 21.28 °C and 31.91‰ respectively. The mactra samples collected have shells which periostracum either have no stripes, or have faint stripes. In most samples a shell surface appears strongly damaged. However, some periostracum areas turned out intact and appear as stained with very dark colour (Fig. 6B-1–3). It was found that this colour is represented by dark brown pigment (Fig. 6B′-1–3). Periferal areas of the shells have similar tone but appear more ligh (Fig. 6B′-1′–3′). A typical dark brown pigment is represented by a piece of periostracum taken from

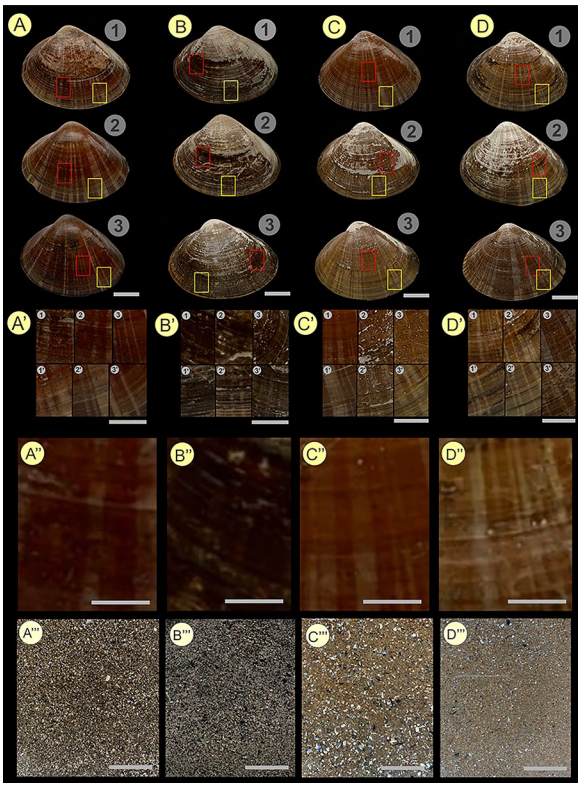

Fig. 6 Shells and samples of the bottom substrate of the bivalve mollusc *Mactra chinensis* collected during SCUBA diving in Peter the Great Bay (Sea of Japan, Russia). **A** three samples (1–3) representing collection in the area 1 (see Fig. 5, 1). **B** three samples (1–3) representing collection in the area 2 (see Fig. 5, 2). **C** three samples (1–3) representing collection in the area 3 (see Fig. 5, 3). **D** three samples (1–3) representing collection in the area 4 (see Fig. 5, 4). **A′** the pigment colour samples tested in the central shell area (red square) and in the peripheral shell area (yellow square) from the samples A1 (**A′**-1, 1′), A2 (**A′**-2, 2′), and A3 (**A′**-3, 3′). **B′** the pigment colour samples tested in the central shell area (red square) and in the peripheral shell area (yellow square) from the samples B1 (**B′**-1, 1′), B2 (B′-2, 2′), and B3 (B′-3, 3′). **C′** the pigment colour samples tested in the central shell area (red square) and in the peripheral shell area (yellow square) from the samples C1 (**C′**-1, 1′), C2 (**C′**-2, 2′), and C3 (**C′**-3, 3′). **D′** the pigment colour samples tested in the central shell area (red square) and in the peripheral shell area (yellow square) from the samples D1 (**D′**-1, 1′), D2 (**D′**-2, 2′), and D3 (**D′**-3, 3′). **A″**–**D″** the pigment colours that are correspondingly typical for the collection areas 1–4. **A‴**–**D‴** the substrate colours that are correspondingly typical for the collection areas 1–4. Scale bar—1 sm (**A**–**D**), (**A‴**–**D‴**); 0.5 sm (**A′**–**D′**); 0.2 sm (**A″**–**D″**)

the central region of the shell of one of the molluscs (Fig. 6B″). The sand of the sea bottom substrate has a dark gray tone (Fig. 6B‴).

In the collection points #3 and #4 that are situated very close to each other (Fig. 5-3, 4) the water temperature and salinity were 21.50 °C/31.75‰ and 21.55 °C/31.32‰ respectively. The shells showed some colour variations (Fig. 6C-1–3, D-1–3).

In the collection point #3 some samples have shells which central parts are stained by very bright foxy pigment (Fig. 6C-1, C′-1). The central areas of the other samples appear not so red and show variants of brown-foxy pigment (Fig. 6C-2, C′-2 and C-3; C′-3). Periferal areas of all shells found in the collection point #3 appear creamy (Fig. 6C′-1′–3′). We reckon that foxy pigment is most specific for molluscs found in collection point #3 (Fig. 6C″).

In the collection point #4 some samples have shells which central parts are stained by creamy colour having slight foxy hue (Fig. 6D-1, 2 and D′-1, 2). We reckon that this colour is most specific for molluscs found in collection point #4 (Fig. 6D″). Periferal areas of all shells found in the collection point #4 appear creamy (Fig. 6D′-1′–3′) and are very close to the colour that is found in peripheral areas of shells found in the collection point #3 (Fig. 6C′-1′–3′). Some samples from the collection points #4 has dark cream tone in both peripheral and central areas (Fig. 6D-3 and D′-3, 3′) but we are not sure that this tone is natural.

The substrate colours differ in the collection points #3 and #4 and could be characterised as a bright-ochroid (Fig. 6C‴) and 'café au lait' (Fig. 6D‴).

Sperm structure analysis

Spermatozoa of *M. chinensis* specimens, representing the three COI clades, look the same at low magnification of scanning electron microscope. All have compact heads and thin flagella (Fig. 7A–C). Analysis of ultrathin sections by transmission electron microscopy showed that mactra sperm can have different acrosomes, the structure of which is presented in two variants. In the first variant, the acrosome consists of two layers, one of which (anterior) is electron-light, and the other (basal) is electron-dense (Fig. 7D–F). In another embodiment, acrosomes have a central electron-dense rod that has an intracellular part inside of the acrosome and external part protruding above the acrosome (Fig. 7G–I). The nucleus always has an oval shape and is filled with electron-dense chromatin (Fig. 7D–I). In the middle part, centrioles are located perpendicular to each other. One of the centrioles is the basal body of the flagellum. Centrioles are surrounded by a mitochondrial ring consisting of four mitochondria (not shown).

Using SEM, it was found that the sperm sets of all studied *M. chinensis* specimens were similar in terms of the presence of common morphological variants. There are spermatozoa with concave acrosomes in which there are no protrusions, as was established when examining the acrosomal surface (Fig. 8A). Such

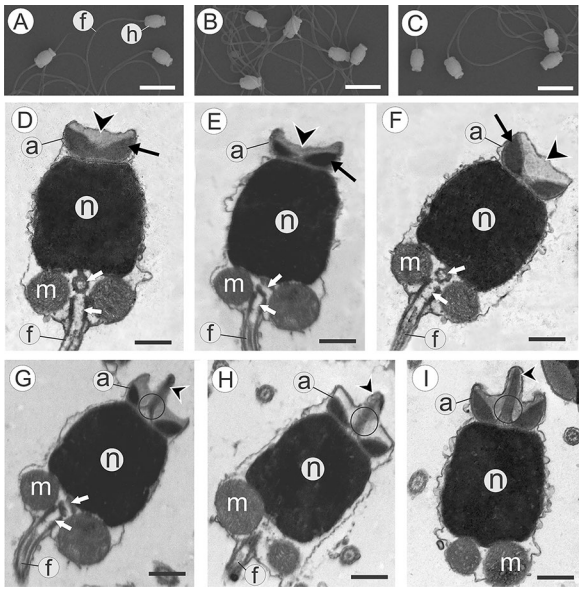

Fig. 7 Spermatozoa of the bivalve mollusc *Mactra chinensis* by scanning electron microscopy (**A**–**C**) and transmission electron microscopy (**D**–**I**). Spermatozoa of *M. chinensis* collected in the Sea of Japan, Russia (**A**), Sea of Japan, South Korea (**B**), Yellow Sea, China (**C**) with a small magnification of an electron scanning microscope; note the head (h) and flagellum (f) that normally constitute sperm cells. The anterior–posterior sperm section projections showing typical intraspecific variations by transmission electron microscopy (**D**–**I**). Note the spermatozoa, which has an acrosome, consisting of two layers, one of which (anterior) is electron-light (arrowheads), and the other (basal) is electron-dense (black arrows), that was found in samples collected in The Sea of Japan, Russia (**D**), The Sea of Japan, South Korea (**E**), Yellow Sea, China (**F**). Note the spermatozoa having an acrosomes with central electron-dense rod that have intracellular part inside of the acrosome (circles), and external part protruding above the acrosome (arrowheads), that were also found in samples collected in The Sea of Japan, Russia (**G**), The Sea of Japan, South Korea (**H**), Yellow Sea, China (**I**). *m* mitochondrion; *n* nucleus; *f* flagellum; the centrioles are showed by white arrows. Scale bar—5 µm (**A**–**C**), 0.5 µm (**D**–**I**)

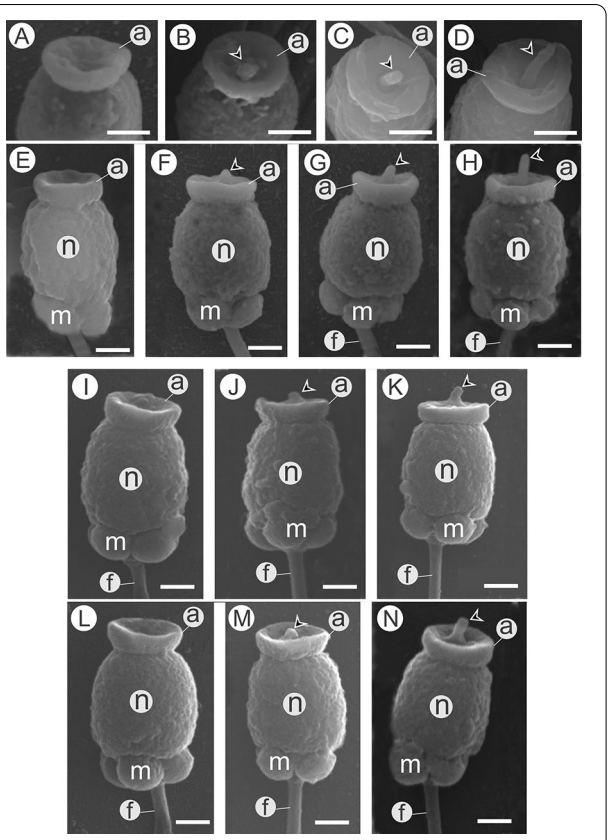

Fig. 8 Spermatozoa of the bivalve mollusc *Mactra chinensis* by scanning electron microscopy. **A**–**H** Spermatozoa of *M. chinensis* collected in the Yellow Sea (China) and belonging to COI clade III. **I**–**K** Spermatozoa *of M. chinensis* collected in the Sea of Japan (Russia) and belonging to COI clade I. **L**–**N** Spermatozoa of *M. chinensis* collected in the Sea of Japan (South Korea) and related to COI clade II. Please note that SPERM1, which has an acrosome without an acrosomal protrusion (**A**, **E**, **I**, **L**), as well as SPERM2, which has an acrosome with an acrosomal protrusion of 0.4 µm long (**B**, **F**, **J**, **M**), and SPERM3, having an acrosome with an acrosomal protrusion of 0.6 µm long (**C**, **G**, **K**, **N**), constitute a universal set of *M. chinensis* spermatozoa. Also note that SPERM4 with acrosomes having a protrusion of 0.8 µm long (**D**, **H**) occurs only in *M. chinensis* collected in the Yellow Sea, China. *a* acrosome; *n* nucleus; *m* mitochondrion; *f* flagellum; arrowheads show acrosomal projections. Scale bar—0.5 µm

spermatozoa with acrosomes without protrusion have been found in molluscs belonging to each of the three COI clades (Fig. 8E, I, L). In some spermatozoa, the acrosomes have a protrusion extending from the center of the acrosomal fossa (Fig. 8B–D, F–H, J–K, M–N).

Calculations performed by analyzing the data obtained using scanning electron microscopy showed that there are three categories of axial rod length. *M. chinensis* representing each of the three clades have spermatozoa with acrosomes, the axial rod of which has a length 0.4 µm (Fig. 8F, J, M), and 0.6 µm (Fig. 8G, K, N). A specific feature of the mactra collected in the Yellow Sea and belonging to COI clade III is the presence of the same three patterns and a fourth sperm pattern with an acrosome, the axial rod length of which reaches 0.8 µm (Fig. 8D, H). Here we characterize sperm patterns as SPERM 1, SPERM 2, SPERM 3, and SPERM 4, respectively.

Quantitative analysis showed that the proportions of sperm samples vary. In COI clade I, the most typical (72%) is SPERM 1. A smaller amount (18%) falls on SPERM 2, and a smaller amount (10%) belongs to SPERM 3 (Fig. 9A). In COI clade II, only 15% falls on SPERM 1. The rest of the spermatozoa is represented by morphs with the numbers of 21% and 64% for SPERM 2 and SPERM 3, respectively (Fig. 9B). In COI clade III,

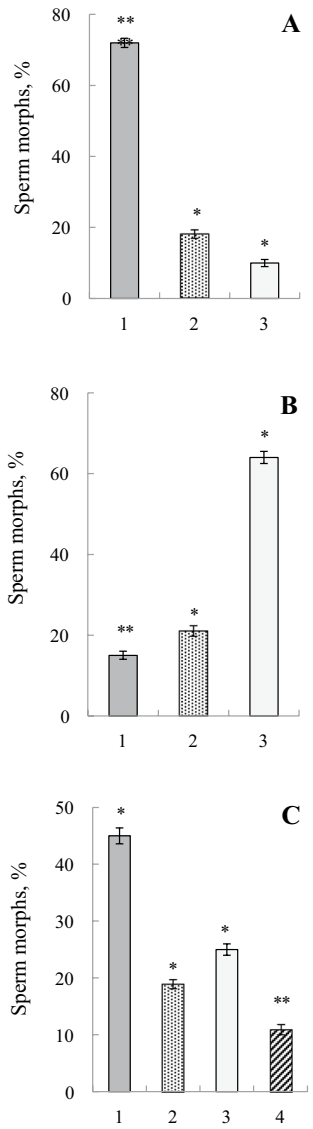

Fig. 9 The bivalve mollusc *Mactra chinensis*. The diagrams show the proportions of sperm morphs that are characteristic for different geographic locations: Sea of Japan, Russia (**A**), Sea of Japan, South Korea (**B**), Yellow Sea, China (**C**). 1—SPERM1, which has an acrosome without an acrosomal protrusion. 2—SPERM2, which has an acrosome with an acrosomal protrusion of 0.4 μm long. 3—SPERM3, having an acrosome with an acrosomal protrusion of 0.6 μm long. 4—SPERM4 with acrosomes having a protrusion of 0.8 μm long. The results were analysed by the Microsoft Excel program. All values are expressed as means with standard error of the mean (SEM). Percentages were calculated using the Student's t test and *P < 0.05, **P < 0.001 were considered statistically significant

the proportions are presented as 45%, 19%, 25% and 11% for SPERM 1, SPERM 2, SPERM 3 and SPERM 4, respectively (Fig. 9C).

Discussion

Genetic divergence of mactrids is a common phenomenon

As shown above, there are three *M. chinensis* genetic lines living in the Asia-Pacific region, specimens of which have been found in the Sea of Japan and the Yellow Sea [15]. Also Ni et al. [20] reported that genetic subdivision occurs in populations of *M. chinensis* in the East China Sea. It is also known about the intraspecific divergence of *Mactra coralline* inhabiting the northern Adriatic coasts of Cesenatico (Italy) [16]. The subdivision of the population into two distinct clades was shown for *M. coralline* habituating in the Gulf of Tunis (northern Tunisia) [21]. Thus, genetic divergence is a common occurrence in mactrids. Mactridae genetic divergence can be triggered by factors such as rivers' outflow, environmental gradient factors and life-history traits [20, 21]. In addition, local hybridization can cause divergence, as shown for other bivalve molluscs [30, 31]. It is obvious that the hybridization process is capable of inducing species collapse [32].

The intraspecific variety of shell coloration exceeds the number of detected species

According to the analysis of shell coloration in genetically tested samples, the coloration of the shell was specific in the representatives of the "Russian", "South Korean" and "Chinese" *M. chinensis* that belong correspondingly to the COI clade I, COI clade II, and COI clade III. Based on this, it would be tempting to speculate that shell coloration follows genetic divergency. However, a study of museum specimens showed that *M. chinensis* is characterized by a wide variety of shell coloration. Museum specimens have never been genetically tested, and the belonging of their shells to one of the discovered species derived from *M. chinensis* could not be genetically confirmed. However, assuming that morphological criteria have always been considered a reliable method for *M. chinensis* identification, we believe that all shells belong to this species complex. Taking into account that the number of types of shell coloration clearly exceeds the number of species diverged from *M. chinensis*, we are confident that none of these species can be distinguished from a single shell pattern.

Individuals belonging to the same genetic clade may have shells of different colors

Further evidence of the impossibility of distinguishing species derived from *M. chinensis* by the only species-specific shell pattern was obtained by genetic analysis of samples from Yantai and Weihai, which have "mustard shells" and "brownish shells", respectively. It turned out that both groups of individuals belong to the same clade (COI clade III) or to the same species *M. chinensis* COI

clade III. Thus, it appears that belonging to the same genetic lineage does not mean uniformity of shell coloration patterns. It seems likely that shell coloration is not optimized by intraspecific genetic divergence, but is regulated by other factors.

The optimization of shell color appears to be the result of environmental influences and gene work

There is evidence that environmental factors influence shell coloration [33, 34]. For example, the geographic distribution of different types of limpet species and the specificity of their shell coloration are determined by the geographic distribution of algae, which are the main dietary component of these molluscs [35]. In *Littorina saxatilis*, salinity exerts an influence on shell colours [36]. Adaptive plasticity of the color of the shell is known in gastropod *Concholepas concholepas*, which adapt it to the color scheme of its victims [37]. Also, the ratio of calcium to magnesium in sea water may affect shell colour hue [17]. The bivalve mollusc *Enigmonia aenigmatica* adapts the shell design to the color of the substrate for camouflage from predators, and it is likely that the substrate affects the color immediately after the larvae have settled [34, 38, 39]. It has been experimentally shown that molluscs are able to change shell color when switching to a new substrate in order to obtain a shell color that better matches the new substrate, and these data support the existence of ecological control of shell coloration [35, 40].

According to some reports, environmental factors can regulate the color of the shell through the work of genes [41–46]. The influence of environmental factors on the genome is mediated by epigenetic mechanisms such as DNA methylation, histone modification, and microRNA expression, which are capable of altering gene expression patterns and causing changes in phenotype [47, 48]. Various types of allelic increase or decrease in gene expression are also associated with epigenetic mechanisms, the activity of which can be determined by external influences [49]. In the bivalve mollusc *Macoma baltica*, four alleles at one locus provide the expression of shell color from white to yellow, orange and red [50]. In Pacific oysters, shell pigmentation is controlled by two genetic loci with two alleles that are responsible for the secretion and distribution of pigments. In addition, one independent locus with two alleles controls striped pigmentation [51]. Thus, it seems possible that the optimization of shell color is the result of the combined work of environmental factors and epigenetic mechanisms.

Shell color is specific and uniform at each collection point

To check if effect of environments on shell coloration could be found in *M. chinensis* we conducted SCUBA-study in four areas of The Peter the Great Bay (Japan Sea) that is known by various environmental conditions [52]. The shell periostarcum of some samples looked damaged but this seems to be normal. Indeed, over time, periostracum decreases in thickness and undergoes erosion being affected by environmental abiotic and biotic factors [53]. However, we were able to find undamaged samples, or we used undamaged pigment areas of partly damaged samples.

We investigated both the central and marginal shell areas. It was often found that marginal shell areas look lighter than central ones. Although in some samples both the central and peripheral areas were almost similar in terms of color density. Anyway, assuming that marginal periostracum is represented by growing area which color is unstable [54], we reckon that exactly central part has mature color.

Remarkable, in the collection points #1 and #2 the samples have a hue that is specific in each collection point. We suggest that shell uniformity found in these niches occurs because of stability of ecologic parameters characteristic for each of these niches. In the points #3 and #4 shell hue was also specific for each collection zone. However, some tone overlap was found in the samples living in these areas. Probably, some shells' colour mixture may occur along the borders of the neighboring niches. Indeed, both collection points (#3 and #4) are situated very close to each other and their borders overlap. Anyway, although more extended SCUBA study is needed to identify the sizes and borders of the niches, we find it possible to speculate that shell color could be considered as a marker specific for each ecological niche that also could be considered as geographical area. It seems likely that the coloration of the shell is the same in a geographic area, the size of which is determined by the zone of action of the ecological features characteristic of the area.

According to our study using SCUBA, the Peter the Great Bay cannot be considered as a single ecological niche inhabited by *M. chinensis* with a single shell coloration. We believe that various ecological niches coexist in the bay and the color of the shells is specific for the niche and is uniform in each niche. Based on the available data, we can distinguish at least six color morphs of *M. chinensis* in the Peter the Great Bay (Fig. 10). However, it is entirely possible that other shell coloration variants could be found.

We found that the color of the substrate was also specific in each area, and noticed that the light/dark color of the substrate corresponded to the light/dark shade of the shells. It was also observed that the presence of brown substrate particles coincided with the brown color of the shell, and the presence of black substrate particles coincided with a darker brown color. This observation

Fig. 10 Intraspecific variations in shell coloration that are typical for the bivalve mollusc *Mactra chinensis* inhabiting Peter the Great Bay (Sea of Japan, Russia). 1—Vostok Bay, Pashinnicov Cape; 2—Russky Island, Vyatlin Cape; 3—Vostok Bay, The Second Priboynaya Bay; 4—Vostok Bay, Voltchanets town; 5—Ussurian Bay; 6—Vostok Bay, The First Priboynaya Bay

suggests the existence of a masking ability of the *M. chinensis* shell color in relation to the substrate.

The quantitative parameters of heterogeneous sets of spermatozoa are specific for each collection site

We also examined whether the structure of the spermatozoa can be used to recognize species derived from *M. chinensis*. By the method of transmission electron microscopy, it was found that the ultrastructure of the spermatozoa of the studied samples corresponds to the ultrastructure of the mactra spermatozoa described in previous studies [55–57]. However, our study by transmission electron microscopy provided more detailed data on the ultrastructure of acrosomes. In the sperm of *M. chinensis* derived species, we found two types of acrosomes, namely, acrosomes without an acrosome protrusion and an acrosome with an acrosome protrusion.

Using scanning electron microscopy, allowing evaluation of external cell shape, we found that in the samples belonging to COI clades I and II, the sperm morphotypes are represented by three variants. These are SPERM 1—sperm with acrosomes without axial rod, SPERM 2—sperm with acrosomes having axial rod with a length corresponding to 0.4 μm, and SPERM 3—sperm with acrosomes having axial rod with a length corresponding to 0.6 μm. Samples belonging to COI Clade III have the same three sperm morphs. In addition, the unique SPERM 4 with an acrosome with a very long axial rod (0.8 μm) was also found in samples of the third clade.

Based on the fact that species derived from *M. chinensis* have more than one sperm morph, these species can be classified as a species with heteromorphic sperm morphology. Interestingly, sperm heteromorphism was recently discovered in another bivalve mollusc, the Pacific oyster *Crassostrea gigas*, whose heteromorphic sperm set consists of six morphologically stable morphs [52]. Targeted research is needed to test whether sperm heteromorphism can be found in other bivalve molluscs.

In animals, the phenomenon of intraspecific heteromorphism of spermatozoa is known [58]. The functional parameters of heterogeneous spermatozoa can vary, for example, higher speed—shorter life span and lower speed—higher life span [59]. There is also a hypothesis that spermatozoa of different phenotypes differ in their allelic content, which ensures differences in sperm competition [60]. In *C. gigas* oysters, in which reproduction occurs by external fertilization in seawater, the causes of sperm plasticity are associated with reproductive adaptation to the aquatic environment, which can be influenced by anthropogenic pollution, intense water current or turbulence, unstable temperature and salinity. The dominant expression of one or another variant of spermatozoa may be associated with a greater degree of adaptability of this variant to a certain type of environment. Parallel expression of additional abundant sperm variants may increase the chances of reproductive success in oysters in unstable conditions [52]. Since *M. chinensis* also has external fertilization a link between environmental conditions and sperm shape seems possible in this species.

Since each of the three *M. chinensis*—derived species have heteromorphic spermatozoa, the validity of these species cannot be confirmed using only one variant of the sperm. However, given that different sperm samples dominated in *M. chinensis* COI clade I and *M. chinensis* COI clade II [15], we hypothesized that the predominant sperm samples could be used as species-specific traits. To check this hypothesis we tested if *M. chinensis* belonging to the COI clade III may have specific dominant sperm morph. This version seemed very likely, given that intraspecific genetic divergence is thought to be accompanied by divergence of sperm structure, as has been shown for some marine invertebrates [61–63]. However, the dominant sperm variant of *M. chinensis* COI clade III was not specific, but coincided with the dominant variant of spermatozoa in the samples belonging to *M. chinensis* COI clade I.

Thus, it can be concluded that the dominant morphs of spermatozoa also cannot be used to identify species descended from *M. chinensis*. However, it should be emphasized that the quantitative parameters of sets of spermatozoa are specific in the Russian, South Korean and Chinese regions. We assume that the parameters of sperm sets are individual in each of the geographic zones, each of which presumably represents an ecological niche that determines the specificity of sperm sets. In other words, we believe that the morphological features of *M. chinensis* male gamete sets are geographically specific.

Geographic identifiers of *M. chinensis* samples can become a means of geo-authentification (= quality control) in the seafood market

In medicinal plants, the type, content and proportion of active substances can vary depending on environmental factors in the areas of plant growth, and, therefore, the geographical identification of plant materials is a necessary measure to control its pharmacological quality [64, 65]. The geographical dependence of the nutritional and medicinal value of species derived from *M. chinensis*, as well as other bivalve molluscs, has not yet been investigated. If future research reveals the dependence of the clam properties on the collection site, the introduction of geographic identifiers will be an effective means of controlling the quality of samples provided by suppliers. Taking into account that the coloration of shells and the structure of spermatozoa in species derived from *M. chinensis* are geographically specific, we propose to use these characters to determine the geographic forms of these species.

We propose geographic identifiers that include information such as: (1) the scientific name of the species (Fig. 11A-1, B-1, C-1), (2) the conventional name of the geographical form of the species (Fig. 11A-2, B-2, C-2), (3) the geographical name of the habitat (cultivation) (Fig. 11A-3, B-3, C-3), (4) geographical coordinates (Fig. 11A-4, B-4, C-4), (5) an image showing the color of the shell (Fig. 11A-5, B-5, C-5), (6) images showing sperm morphs (Fig. 11A-6, B-6, C-6), (7) proportional ratio of sperm morphs with an indication of the dominant type of sperm (Fig. 11A-7, B-7, C-7), (8) a scientific source on the basis of which an idea of the geographical form of the species was created (Fig. 11A-8, B-8, C-8). Using these identifiers, it will be possible to (i) determine the geographical origin of the molluscs by simply comparing the colors of the shells, and (ii) control the geographical origin through sperm examination, which can be performed in an electron microscopy laboratory. An expanded study of the *M. chinensis* species complex

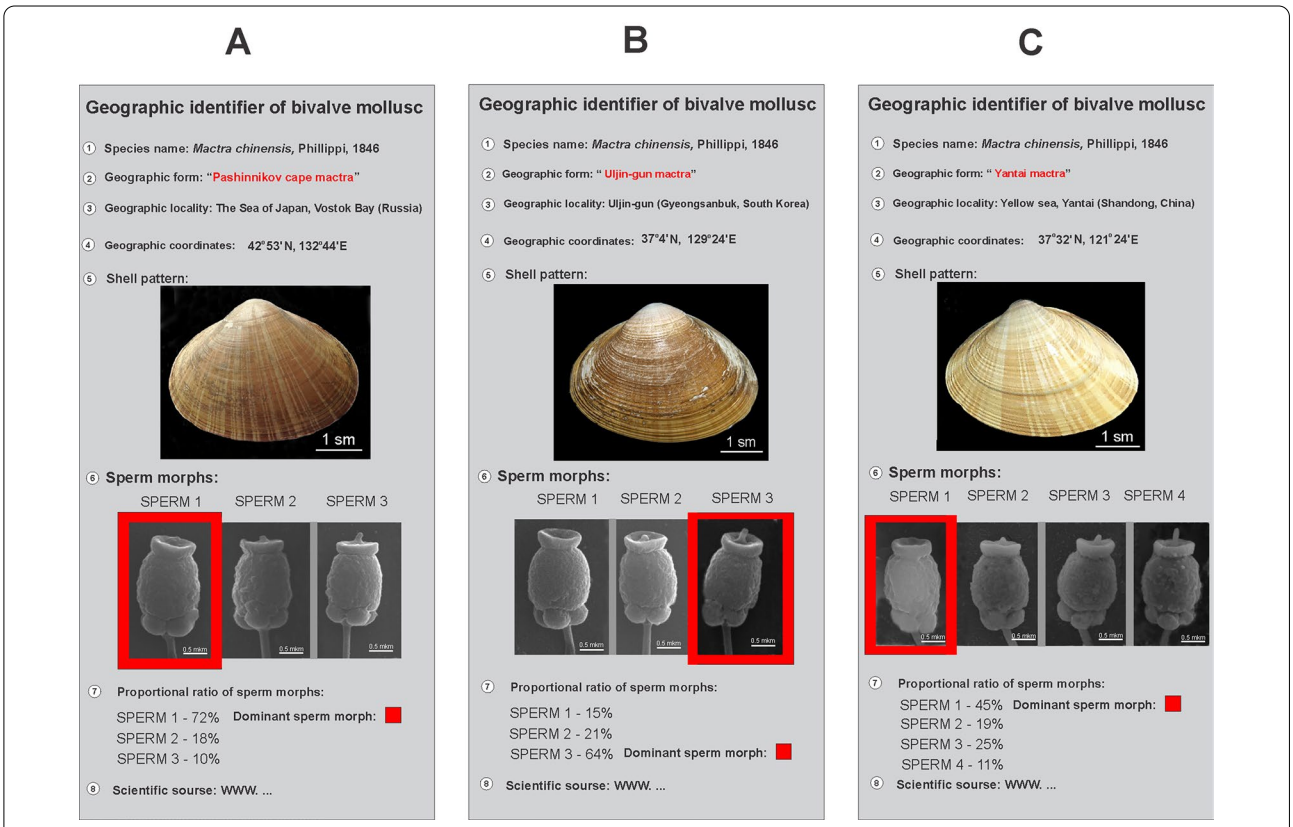

Fig. 11 Identifiers of geographical forms of the bivalve mollusc *Mactra chinensis*, in which shell coloration and parameters of sperm sets are used as morphological criteria. Identifiers include information such as: (1) scientific name of the species (**A**-1, **B**-1, **C**-1), (2) conventional name of the geographical form of the species (**A**-2, **B**-2, **C**-2), (3) geographic locality (**A**-3, **B**-3, **C**-3), (4) geographic coordinates (**A**-4, **B**-4, **C**-4), (5) an image showing the color of the shell (**A**-5, **B**-5, **C**-5), (6) the images showing sperm morphs (**A**-6, **B**-6, **C**-6), (7) proportional ratio of sperm morphs with an indication of the dominant sperm morph showed by red squares (**A**-7, **B**-7, **C**-7), (8) scientific source on the basis of which an idea of the geographical form of the species was created (**A**-8, **B**-8, **C**-8). Note the red square in Section 6, which indicates the sperm morph that dominates in the geographic form of the mollusc

in the Asia-Pacific region is needed to provide detailed identifiers that will become a reliable tool for tracing the origin of these valuable molluscs in seafood markets.

Conclusions

When testing the mitochondrial COI gene, it was revealed that the bivalve mollusc *M. chinensis*, which lives in the Asia-Pacific region, diverged into three species. It was found that these species cannot be reliably determined based on analysis of the shell coloration and sperm structure due to the plasticity of these morphological characters. However, since the coloration of the shells and the quantitative parameters of sperm sets are geographically specific, the geographic identification of *M. chinensis* forms seems possible using these characters. It is proposed to introduce geographical identifiers to control the geographical origin of the clams in seafood markets.

Acknowledgements
This project supported by the FEB RAS Grants (N 12-I-P30-10 for Dr. Arkadiy Reunov and N 12-I-P6-04 for Dr. Andrey Adrianov), the Russian Government support (Grant N 11. G 34.31.0010), by the program for fundamental research "The Far East", (Project No. 15-I-6-007_o), by the International Science Partnership Program of the Chinese Academy of Science (No. 133137KYSB20200002), and by the Special Funds for the Young Scholars of Taxonomy of the Chinese Academy of Sciences (No. ZSBR-009). DNA barcoding analysis was supported in part by the International Barcode of Life project funded by Genome Canada through Ontario Genomics Institute. We are grateful to Andreia Salvador (Natural History Museum, London, UK) for sending us photographs of the syntype of *Mactra sulcataria* and Irina Volvenko (Zoological Museum, Far Eastern Federal University, Vladivostok, Russia) for assistance in photographic work. Many thanks to Diving Department Head A. Goloseev and to divers N. Prohorov, K. Dudka, A. Oskolkov, M. Eremenko, I. Krasilnikov, S. Izrailskiy (National Scientific Centre of Marine Biology, Vladivostok, Russia) for very professional collection of *M. chinensis*. Many thanks to Elizabeth Alexandrov for photographing mollusc shells. We are deeply indebted to Denis Fomin for the helpful assistance during observations with the scanning electron microscope and transmission electron microscope in the Microscopy Core Facility of the National Scientific Centre of Marine Biology (Vladivostok, Russia). A part of the electron microscopy study was done by Dr. Arkadiy Reunov in the Microscopy Facility at St. Francis Xavier University (Antigonish, NS, Canada).

Authors' contributions
All authors read and approved the final manuscript.

Funding
This project supported by the FEB RAS Grants (N 12-I-P30-10 for Dr. Arkadiy Reunov and N 12-I-P6-04 for Dr. Andrey Adrianov), the Russian Government support (Grant N 11. G 34.31.0010), by the Program for Fundamental Research "The Far East", (Project No. 15-I-6-007_o), by the International Science Partnership Program of the Chinese Academy of Science (No. 133137KYSB20200002), and by the Special Funds for the Young Scholars of Taxonomy of the Chinese Academy of Sciences (No. ZSBR-009).

Availability of data and materials
The datasets generated and analysed during the current study are available from the corresponding author on request, and will be available in ResearchGate after publication of the article.

Declarations

Ethics approval and consent to participate
Collection was performed under appropriate collection protocols.

Consent for publication
Not applicable.

Competing interests
The authors declare that they have no competing interests.

Author details
[1]Department of Biology, St. Francis Xavier University, Antigonish NS B2G 2W5, Canada. [2]National Scientific Center of Marine Biology, Far Eastern Branch, Russian Academy of Sciences, Vladivostok 690041, Russia. [3]Department of Marine Organism Taxonomy and Phylogeny, Institute of Oceanology, Chinese Academy of Sciences, 7 Nanhai Road, Qingdao 266071, China. [4]Canadian Centre for DNA Barcoding, Biodiversity Institute of Ontario, Guelph, Canada. [5]School of Natural Sciences, Far Eastern Federal University, 10 Ajax Bay, Russky Island, Vladivostok 690950, Russia.

Received: 19 November 2020 Accepted: 15 October 2021
Published online: 30 October 2021

References

1. Xu F. Bivalve Mollusca of China seas. Beijing: Science Press; 1997.
2. Yavnov SV. Atlas of bivalve mollusks of the far eastern seas of Russia. Vladivostok: Dyuma; 2000. p. 167.
3. Higo S, Callomon P, Goto Y. Catalogue and bibliography of the marine shell-bearing Mollusca of Japan. Type figures. Osaka: Elle Scientific Publications; 2001.
4. Kwon OK, Min DK, Lee JR, Lee JS, Je JG, Choe BL. Korean mollusks with color illustrations. Busan: Hanguel; 2001.
5. Lutaenko KA. Bivalve mollusks of Ussuriysky Bay (Sea of Japan). Part 1 Bull Russ Far East Malacol Soc. 2005;9:59–81.
6. Evseev GA, Yakovlev YM. The bivalve molluscs of far eastern seas of Russia. Vladivostok: Polikon; 2006.
7. Xu F, Zhang S. An illustrated Bivalvia Mollusca fauna of China seas. Beijing: Science Press; 2008.
8. Huber M. Compendium of bivalves. A full-color guide to 3300 of the world's marine bivalves. A status on Bivalvia after 250 years of research. Hackenheim: ConchBooks; 2010.
9. Lutaenko KA, Noseworthy RG. Catalogue of the living Bivalvia of the continental coast of the Sea of Japan (east sea). Vladivostok: Dalnauka; 2012.
10. Lutaenko KA, Volvenko IE, Adrianov AV. Atlas of common bivalve mollusks of Peter The Great Bay (Sea of Japan). Vladivostok: Far Eastern Federal University; 2017.
11. Sakurai I, Horii T, Murakami O, Nakao S. Population dynamics and stock size prediction for the sunray surfclam *Mactra chinensis* at Tomakomai, southwest Hokkaido, Japan. Fish Bull. 1998;96:344–51.
12. Ni L, Li Q, Kong L. Microsatellites reveal fine-scale genetic structure of the Chinese surf clam *Mactra chinensis* (Mollusca, Bivalvia, Mactridae) in Northern China. Mar Ecol. 2011;32:488–97.
13. Higashi K, Takeda K, Mukuno A, Okamoto Y, Masuko S, Linhardt RJ, Toida T. Identification of keratan sulfate disaccharide at C-3 position of glucuronate of chondroitin sulfate from *Mactra chinensis*. Biochem J. 2016;473(22):4145–58.
14. Caterson B, Melrose J. Keratan sulfate, a complex glycosaminoglycan with unique functional capability. Glycobiology. 2018;28(4):182–206.
15. Reunov AA, Lutaenko KA, Zakharov EV, Vekhova EE, Reunova YA, Alexandrova YN, Sharina SN, Adrianov AV. Disproportional heteromorphism of male gametes in the bivalve mollusk *Mactra chinensis* is related to genetic divergence of this species. Dokl Biol Sci. 2014;455(1):132–5.
16. Guarniero I, Plazzi F, Bonfitto A, Rinaldi A, Trentini M, Passamonti M. The bivalve mollusk *Mactra coralline*: genetic evidence of existing sibling species. J Mar Biol Assoc UK. 2010;90:633–44.
17. Williams ST. Molluscan shell colour. Biol Rev. 2017;92(2):1039–58.
18. Marks JA, Biermann CH, Eanes WF, Kryvi H. Sperm polymorphism within the sea urchin *Strongylocentrotus droebachiensis*: divergence between Pacific and Atlantic Oceans. Biol Bull. 2008;215:115–25.
19. Ni L, Li Q, Kong L, Huang S, Li L. DNA barcoding and phylogeny in the family Mactridae (Bivalvia: Heterodonta): evidence for cryptic species. Biochem Syst Ecol. 2012;44:164–72.

20. Ni G, Li Q, Ni L, Kong L, Yu H. Population subdivision of the surf clam *Mactra chinensis* in the East China Sea: Changjiang River outflow is not the sole driver. PeerJ. 2015;3:e1240.
21. Chetoui I, Denis F, Boussaid M, Telahigue K, El Cafsi M. Genetic diversity and phylogenetic analysis of two Tunisian bivalves (Mactridae) *Mactra corallina* (Linnaeus, 1758) and *Eastonia rugosa* (Helbling, 1799) based on COI gene sequences. C R Biol. 2016;339:115–22.
22. Plazzi F, Passamonti M. Towards a molecular phylogeny of Mollusks: bivalves' early evolution as revealed by mitochondrial genes. Mol Phylogenet Evol. 2010;57(2):641–57.
23. Puillandre N, Lambert A, Brouillet S, Achaz G. ABGD, automatic barcode gap discovery for primary species delimitation. Mol Ecol. 2012;21(8):1864–77.
24. Kumar S, Stecher G, Li M, Knyaz C, Tamura K. MEGA X: molecular evolutionary genetics analysis across computing platforms. Mol Biol Evol. 2018;35(6):1547–9.
25. Kimura O. A simple model for estimating evolutionary rates of base substitutions through comparative studies of nucleotide sequences. J Mol Evol. 1980;16:111–20.
26. Darriba D, Taboada GL, Doallo R, Posada D. jModelTest 2: more models, new heuristics and parallel computing. Nat Methods. 2012;9(8):772–772.
27. Ronquist F, Teslenko M, Mark PVD, Ayres DL, Darling A, Höhna S, Larget B, Liu L, Suchard MA, Huelsenbeck JP. MrBayes 3.2: efficient Bayesian phylogenetic inference and model choice across a large model space. Syst Biol. 2012;61(3):539–42.
28. Stamatakis A. RAxML version 8: a tool for phylogenetic analysis and post-analysis of large phylogenies. Bioinformatics. 2014;30:1312–3.
29. Saitou N, Nei M. The neighbor-joining method: a new method for reconstructing phylogenetic trees. Mol Biol Evol. 1987;4(4):406–25.
30. Skurikhina LA, Kartavtsev YF, Chichvarkhin AY, Pankova MV. Study of two species of mussels, *Mytilus trossulus* and *Mytilus galloprovinciallis* (Bivalvia: Mytilidae), and their hybrids in Peter the Great Bay of the Sea of Japan with the use of PCR markers. Genetika. 2001;37:1717–20.
31. Brannock PM, Wethey DS, Hilbish TJ. Extensive hybridization with minimal introgression in *Mytilus galloprovincialis* and *M. trossulus* in Hokkaido, Japan. Mar Ecol Prog Ser. 2009;383:161–71.
32. Nilsson PA, Hulthén K, Chapman BB, Hansson L-A, Brodersen J, Baktoft H, Vinterstare J, Brönmark C, Skov C. Species integrity enhanced by a predation cost to hybrids in the wild. Biol Lett. 2017;13:20170208.
33. Stanley SM. Relation of shell form to life habits in the Bivalvia (Mollusca). Geol Soc Am Mem. 1970;125:1–296.
34. Moss SM. *Enigmonia aenigmatica*: an enigmatic Molluscan chameleon. The marine biology of the South China Sea. In: Morton B, editor. Proceedings of the first international conference of the marine biology of Hong Kong and the South China sea, Hong Kong, 28 October–3 November 1990. Hong Kong: Hong Kong University Press; 1990.
35. Lindberg DR, Pearse JS. Experimental manipulation of shell color and morphology of the limpets *Lottia asmi* (Middendorff) and *Lottia digitalis* (Rathke) (Mollusca: Patellogastropoda). J Exp Mar Biol Ecol. 1990;140:173–85.
36. Sokolova IM, Berger VJ. Physiological variation related to shell colour polymorphism in White Sea *Littorina saxatilis*. J Exp Mar Biol Ecol. 2000;245(1):1–23.
37. Manríquez PH, Lagos NA, Jara ME, Castilla JC. Adaptive shell color plasticity during the early ontogeny of an intertidal keystone snail. Proc Natl Acad Sci USA. 2009;106:16298–303.
38. Morton B. The biology, ecology and functional aspects of the organs offeeding and digestion of the S.E. Asian mangrove bivalve, *Enigmonia aenigmatica* (Mollusca: Anomiacea). J Zool Lond. 1976;179:437–66.
39. Sigurdson JB, Sundari G. Shellular changes in the colour in the tree-climbing bivalve *Enigmonia aenigmatica* (Holten 1802) (Annomiidae). Raffles Bull Zool. 1990;38:213–8.
40. Gain AJ. The colours of marine bivalve shells with special reference to *Macoma balthica*. Malacologia. 1988;28:289–318.
41. Brake J, Evans F, Langdon C. Evidence for genetic control of pigmentation of shell and mantle edge in selected families of Pacific oysters, *Crassostrea gigas*. Aquaculture. 2004;229:89–98.
42. Hu Z, Song H, Zhou C, Yu ZL, Yang MJ, Zhang T. De novo assembly transcriptome analysis reveals the preliminary molecular mechanism of pigmentation in juveniles of the hard clam *Mercenaria mercenaria*. Genomics. 2020;112(5):3636–4364.
43. Bonnard M, Cantel S, Boury B, Parrot I. Chemical evidence of rare porphyrins in purple shells of *Crassostrea gigas* oyster. Sci Rep. 2020;10:12150.
44. Lemer S, Saulnier D, Gueguen Y, Planes S. Identification of genes associated with shell color in the black-lipped pearl oyster, *Pinctada margaritifera*. BMC Genom. 2015;16:568.
45. Mao J, Zhang X, Zhang W, Tian Y, Wang X, Hao Z. Genome-wide identification, characterization and expression analysis of the MITF gene in Yesso scallops (*Patinopecten yessoensis*) with different shell colors. Gene. 2019;688:155–62.
46. Yue X, Nie Q, Xiao G, Liu B. Transcriptome analysis of shell color-related genes in the clam *Meretrix meretrix*. Mar Biotechnol. 2015;17:364–74.
47. Handy ED, Castro R, Loscalzo J. Epigenetic modifications: basic mechanisms and role in cardiovascular disease. Circulation. 2011;123(19):2145–56.
48. Yao Q, Chen Y, Zhou X. The roles of microRNAs in epigenetic regulation. Curr Opin Chem Biol. 2019;51:11–7.
49. Wang H, Lou D, Wang Z. Crosstalk of genetic variants, allele-specific DNA methylation, and environmental factors for complex disease risk. Front Genet. 2019;9:695.
50. Luttikhuizen PC, Drent J. Inheritance of predominantly hidden shell colours in *Macoma balthica* (L.) (Bivalvia: Tellinidae). J Molluscs Stud. 2008;74:363–71.
51. Xu C, Li Q, Yu H, Liu S, Kong L, Chong J. Inheritance of shell pigmentation in Pacific oyster *Crassostrea gigas*. Aquaculture. 2019;512:734249.
52. Reunov AA, Vekhova EE, Zakharov EV, Reunova YA, Alexandrova YN, Sharina SN, Adrianov AV. Variation of sperm morphology in Pacific oyster precludes its use as a species marker but enables intraspecific geoauthentification and aquatic monitoring. Helgol Mar Res. 2018;72:8.
53. Guenther J, Southgate PC, De Nyc R. The effect of age and shell size on accumulation of fouling organisms on the Akoya pearl oyster *Pinctada fucata* (Gould). Aquaculture. 2006;253(1–4):366–73.
54. Popov SV. Formation of bivalve shells and their microstructure. Paleontol J. 2014;48(14):1519–31.
55. Kim JH, Yoo MS. Spermatozoan ultrastructure in four species of Mactridae. J Korean Fish Soc. 2002;35:504–11.
56. Tyurin SA, Drozdov AL. Ultrastructure of sperm in *Mercenaria stimpsoni* and *Mactra chinensis* (Mollusca: Bivalvia) from the Sea of Japan. Russ J Mar Biol. 2005;31:391–5.
57. Chung EY, Kim EJ, Park GM. Spermatogenesis and sexual maturation in male *Mactra chinensis* (Bivalvia: Mactridae) of Korea. Integr Biosci. 2007;11(2):227–34.
58. Morrow EH, Gage MJG. Consistent significant variation between individual males in spermatozoal morphometry. J Zool. 2001;254(2):147–53.
59. Levitan D. Sperm velocity and longevity trade off each other and influence fertilization in the sea urchin *Lytechinus variegates*. Proc R Soc Lond B. 2000;267:531–4.
60. Borowsky R, Luk A, He X, Kim RS. Unique sperm haplotypes are associated with phenotypically different sperm subpopulations in Astyanax fish. BMC Biol. 2018;16:72.
61. Landry C, Geyer LB, Arakaki T, Uehara T, Palumbi SR. Recent speciation in the Indo-West Pacific: rapid evolution of gamete recognition and sperm morphology in cryptic species of sea urchin. Proc R Soc Lond. 2003;270:1839–47.
62. Arakaki Y, Uehara T. Morphological comparison of black Echinometra individuals among those in the Indo-West Pacific. Zoolog Sci. 1999;16:551–8.
63. Geyer LB, Palumbi SR. Reproductive character displacement and the genetic of gamete recognition in tropical sea urchins. Evolution. 2003;57(5):1049–60.
64. Liu W, Liu J, Yin D, Zhao X. Influence of ecological factors on the production of active substances in the anti-cancer plant *Sinopodophyllum hexandrum* (Royle) T.S. Ying. PLoS ONE. 2015;10(4):e0122981.
65. Reunov AA, Reunova GD, Atopkin DM, Reunova YA, Muzarok TG, Zakharov EV, Zhuravlev YN. The identification of Araliaceae species by ITS2 genetic barcoding and pollen morphology. Planta Med. 2018;84(01):42–8.

Publisher's Note